Spectral colour changes: a promising parameter for smart flax dew retting monitoring solutions

Suvajit Mukherjee, Dmitry Galinousky, Anne- Sophie Blervacq, Lionel Buchaillot, Steve Arscott, Sébastien Grec

Computers and Electronics in Agriculture 243 (2026) 111407

Contents lists available at ScienceDirect

Computers and Electronics in Agriculture

journal homepage: www.elsevier.com/locate/compag

Spectral colour changes: a promising parameter for smart flax dew retting monitoring solutions

Suvajit Mukherjee [a,*], Dmitry Galinousky [a,1], Anne- Sophie Blervacq [a], Lionel Buchaillot [b], Steve Arscott [b], Sébastien Grec [a,c,d,**]

[a] Univ. Lille, CNRS, UMR 8576 - UGSF - Unité de Glycobiologie Structurale et Fonctionnelle, F-59000 Lille, France
[b] Univ. Lille, CNRS, Centrale Lille, Univ. Polytechnique Hauts-de-France, UMR 8520 - IEMN - Institut d'Electronique de Microélectronique et de Nanotechnologie, F-59000 Lille, France
[c] Inserm U1285, Univ. Lille F-59000 Lille, France
[d] CHU Lille, Laboratoire de Parasitologie-Mycologie, F-59000 Lille, France

ARTICLE INFO

Keywords:
Flax dew retting
Colour scale
Spectro-colorimetry
Smart sensor
Agriculture 4.0

ABSTRACT

Natural fibres from plants such as flax (*Linum usitatissimum*) are gaining interest as possible green replacements of synthetic fibres to reduce textile pollution footprints. However, the extraction-facilitating process of bast fibres from the flax stem, i.e. dew retting, is still empirically evaluated, resulting in either over or under retted fibre, both of which decrease the resulting fibre quality and introduce batch variability. There is currently no in-the-field device available to help farmers to monitor and manage flax dew retting. Flax growers generally use a 'Fried-test' or 'organoleptic' evaluations to define dew retting progression. In this study, we have measured this stem surface colour change using a spectrophotometer. Spectra in 400 to 700 nm range were acquired during 3 retting periods, carried out in different retting years, involving 4 fields in total. Cluster analysis of spectra revealed four distinct stages of retting which we termed: beginning, early, middle and advanced. Moreover, by the use of a statistical pipeline including PCA and PLS-DA we established that measurements of only four selected wavelengths (480, 490, 600, and 610 nm) are sufficient to predict the retting stage with a high degree of confidence. This work paves the way for the future development of colour sensors, which could be mounted on drones. Such onboard sensors would provide farmers with a practical tool to identify the optimal moment to end retting.

1. Introduction

Natural fibres from various plant species have been used by humans for centuries to create robust textiles, and more recently as a sustainable alternative to synthetic fibres in composite materials (Melelli et al., 2021; Tariq et al., 2022). Bast fibres of flax (*Linum usitatissimum* L.) are mid-long to long and dense in crystalline cellulose i.e., strong and flexible (Thapliyal et al., 2023). They are particularly suitable to make high-quality textiles and various composite products (Mohanty et al., 2000; Chand and Fahim, 2020). Firstly, the fibres are pre-extracted following a process called retting (Elfaleh et al., 2023; Mukherjee et al., 2025). Then extraction involves mechanical scutching, combing, spinning (Gomez-Campos et al., 2021). Retting is a microbial process where the stem tissue surrounding the bast-fibre bundles are disaggregated by the enzymatic action of microorganisms from soil and phyllosphere in humid conditions (Djemiel et al., 2017). In Europe, the most common method of retting is 'dew retting' (Chabbert et al., 2020; Réquilé et al., 2021). This involves leaving the harvested flax plants in the field for several weeks, where they are exposed to night-time dew, daytime sun and rainfall. These conditions promote the growth of

Abbreviations: Anova, Analysis of variance; AUC, Area under the curve; CIE Lab, Commission Internationale de l'Éclairage L*a*b*; CIM, Cluster image mapping; HSD, Honestly significant difference; IQR, Interquartile range; ND15, Normalized days at 15° C; PCA, Principal component analysis; PLS DA, Partial least squares discriminant analysis; ROC, Receiver operating characteristic; SCI, Specular component included; WSS, Within-cluster sum of squares.

* Corresponding author at: INRAE, UR 1268 - BIA - Unite Biopolymeres, Interactions, Assemblages, F-44316 Nantes, France.
** Corresponding author at: Univ. Lille, CNRS, UMR 8576 - UGSF - Unité de Glycobiologie Structurale et Fonctionnelle, F-59000 Lille, France
E-mail addresses: suvajit.mukherjee@inrae.fr (S. Mukherjee), sebastien.grec@univ-lille.fr (S. Grec).
[1] Current address: Univ. Lille, INSERM UMR 1011 - Integrated molecular analysis of liver diseases, F-59045 Lille, France.

https://doi.org/10.1016/j.compag.2026.111407
Received 3 July 2025; Received in revised form 16 December 2025; Accepted 2 January 2026
Available online 9 January 2026

microorganisms on and within the flax stems which causes the enzymatic degradation of the cell wall polymers such as pectin and hemicellulose (Wang et al., 2017; Mukherjee et al., 2024; Mukherjee et al., 2025). Degradation of these cementing materials during dew retting facilitates the release of the cellulosic fibres from other stem tissues and from each other (Meijer et al., 1995; Bourmaud et al., 2019). As a consequence, fibres become easier to separate during subsequent mechanical extraction steps so that good quality technical fibres are obtained (Baley, 2002; Akin, 2013; Bourmaud et al., 2019). Nonetheless, a prolonged dew-retting or over-retting can cause the degradation of cellulosic fibres, impacting the mechanical quality (Brown et al., 1984; Bratt et al., 1988; Meijer et al., 1995). On the other hand, under-retted fibres are not easily separated from the stem tissue, often causing cuticle/woody particles contamination reducing the fibre quality in fineness and homogeneity (Akin, 2013). Despite significant progress in recent years in understanding the chemical and biological mechanisms of dew retting (Djemiel et al., 2017; Bourmaud et al., 2019; Chabbert et al., 2020; Mukherjee et al., 2024), there is no methodology based on a reliable device for assessing the progression of this process. This leads industries and farmers to decide when to stop retting processing based on empirical assessments drawn from their experience. Farmers often rely on the straw colour change or manual in-hand evaluation of ease of fibre separation (Fried's test) to decide to stop retting (Akin et al., 1996; Henriksson et al., 1997; Martin et al., 2013). Several studies, attempting to produce a tool to test the degree of retting using both physical (Seaby and Mercer, 1984; Brown et al., 1986; Donaghy et al., 1992; Meijer et al., 1995; Sharma and Faughey, 1999) and biochemical properties (Meijer et al., 1995; Sharma and Faughey, 1999), suggested that a more sensitive and multimodal method is needed to determine and monitor the degree of retting in the field. Amongst others, monitoring of stem surface colour during dew-retting could represent a very promising parameter that could be easily measured with a reliable instrument in a non-destructive way. Flax stem colour change, inter alia, is commonly used by farmers to qualitatively evaluate the degree of retting; however, the scientific literature is scarce regarding quantitative studies of colour change of retting flax stems. These studies, often limited to visual or CIE Lab colour space (Commission Internationale de l'éclairage – L*a*b*) (Bleuze et al., 2018; Chabbert et al., 2020, 2023; Peyrache et al., 2024), indicate that colour change occurs with progression of retting but do not associate a specific wavelength with the degree of retting. In this study, we will examine, for the first time, colour changes across the entire visible spectrum with a view to identify wavelengths that can be considered as reliable markers. Such markers could serve as a basis for developing sensors to monitor retting directly in the field.

2. Materials and methods

2.1. Experimental design, sampling and data collection

Flax stems were harvested over three years (2014, 2021 and 2022) from four different fields (named A to D) in north of France, where retting was carried out by experts (flax growers) (Fig. 1**(a)**). Samples were collected from 3 − 5 sampling spots (150 × 100 cm) representing biological replicates (named T1-T3 or T5) for each field/ time point (days). Each sample consisted of a bundle of ~ 50–60 stems, grouped together for colour spectrum measurement (Fig. 1**(b)**). Extra-retted samples were collected from field D in 2022. In that case, the retting process finished on day 55 after plants were uprooted, when farmers decided to collect the straw from the field to perform scutching. Residual samples were kept on the field D for extra-retting and collected on day 69 and day 90. Details about sampling, cultivars and data sets are provided in Table 1 and Fig. 1**(a).** All field-collected samples were either naturally dry or air-dried at room temperature (20–21 °C, 60–65 % RH) for one or two days (until visually dry). In 2014 and 2021, samples were labelled by retting day and stored in the dark at room temperature until spectral analysis, while 2022 samples were subjected to spectral analysis along with sampling. Weather information during field retting was obtained from the nearby weather stations (https://www.infoclimat.fr). Normalized days at 15 °C (ND15) were calculated following Thiebeau and Recous, 2017; Réquilé et al., 2021, with formula: $ND15 = 25/(1 + 145 \times \exp(-0.120 \times T°))$, where T° denotes daily mean temperature. Cumulative rainfall, cumulative temperature and cumulative ND15 are provided in **Supplementary Data 3**. Soil samples were collected from fields A, B and C for all replicates and sent to the "Laboratoire d'Analyses des Sols d'Arras, ***INRAE*** (https://las.hautsdefrance.hub.inrae.fr/prestations)" to assess the soil composition (**Supplementary** Fig. 2; **Supplementary Data 3**). Field A is a silty-sandy soil with low clay (15 %) and organic carbon (11 $g \cdot kg^{-1}$), typical of a neutral to slightly acidic pH. In contrast, field B and C are finer silty-clay soils with higher clay content (26–31 %), greater organic carbon (20–23 $g \cdot kg^{-1}$), and neutral to slightly alkaline pH, with field C being the most clayey and calcareous.

2.2. Collection of spectral readings

Colour changes in flax stem surface during retting were measured using a portable spectrophotometer (CM-23d, Konica Minolta), which was calibrated following the suppliers' guidelines. The specular component included (SCI) mode of the spectrophotometer was used to capture readings across the visual spectrum (400–700 nm) with 10 nm intervals. SCI is a better choice for sample-to-sample comparison as it includes diffuse and specular reflections from the stems (Sanderson, 2015). CIE Lab values were also acquired with the same spectrophotometer for an alternative variant of the optical data representation. Data was processed using SpectraMagicNX software (www.konicaminolta.fr, 2021). Measurements were taken at five positions along each flax stem bundle (following a contact-based approach): two measurements at the top and bottom of the bundle, and one at the middle (Fig. 1 **(b), (c)**). All recordings were first grouped based on their position on the stem (Top, Middle, Bottom), across the biological replicates (T_1 to T_3 or T_5) and then averaged (Fig. 1**(b)**). This approach yielded 9 to 15 averaged readings per retting time point, depending on dataset and sampling structure (**Supplementary Data 1b**). Averaged recordings were then normalized by the use of the TotIn procedure of the chemospec (v.6.1.10) R package (**Supplementary Fig. 3, Supplementary Data 2**).

Photographs provided in **Supplementary Fig. 4**, illustrating the colour changes, were taken by a NIKON D5000 camera (24 megapixels, f/4.8 aperture) using auto settings (ISO 400, exposure time 1/90 s) under indoor lighting at a 90° angle.

2.3. Statistical analysis

All statistical analyses were carried out in R software (https://www.r-project.org/, version 4.4.2, 2024–10-31).

Concerning CIE Lab colour space analysis, outlier values identified by inter quartile range (IQR) were removed. Then the Shapiro-Wilk test was used to check for normal distribution of data and to check for equal variances among groups the Levene's test was used. A one-way analysis of variance (ANOVA) along with Tukey's HSD (Honestly Significant Difference) test was performed using the *Stats* R package (v.4.4.2).

Concerning the spectral SCI data, averaged spectra readings were first normalized. Number of sample groups (defining "retting stages") was estimated by K-means clustering using inbuilt *Stats* (v.4.4.2) package in R. The elbow plot was used to plot within-cluster sum of squares (WSS) to evaluate the optimal number of clusters and the resulting cluster assignments were visualized with the *factoextra* R package.

Unsupervised Principal Component Analysis (PCA-analysis) and supervised Partial Least Squares Discriminant Analysis (PLS-DA) methods were used for data reduction. Both methods were performed using the mixOmics R package (v.6.30.0) (https://www.r-project.org/) (Rohart et al., 2017). Model robustness was assessed using 10-fold repeated cross-validation (10 repeats) with the *caret* (v.7.0.1) package (*method* = *"pls"*). Class separation and feature contribution were examined

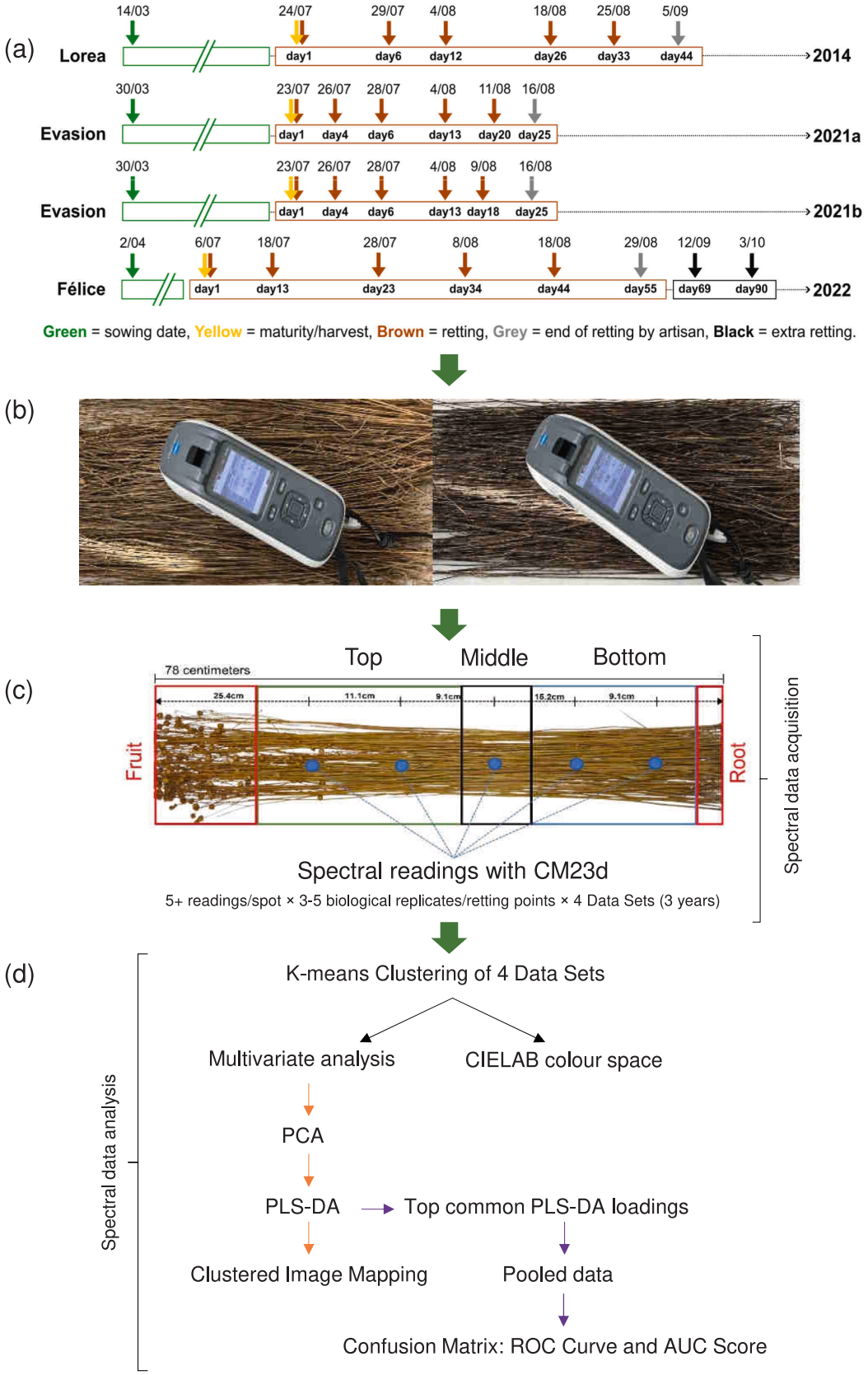

Fig. 1. Experimental design of flax stem surface colour analysis during retting. (a) Crop management diagram of retting events. (b) Surface colour acquisition of flax stems during the retting, with the CM-23d portable spectrophotometer (Konika-Minolta). (c) Spectral data acquisition and (d) data analysis pipeline.

Table 1
Four data sets metadata.

Datasets	Year	Cultivar	Locations & GPS coordinates	Sampling Date	Cumulative Days*	Cumulative Normalized Days at 15°C	Cumulative Rains (mm)
A	2014	Lorea	Martainneville	24-Jul	1	0	0
			50°00′03″N, 1°42′27″E	29-Jul	6	8.5	17.4
				4-Aug	12	17.2	26.9
				18-Aug	26	34.7	109.8
				25-Aug	33	41	166.6
				5-Sep	44	55.7	175.4
B	2021	Evasion	Bavinchove	23-Jul	1	0	0
			50°47′05.5″N, 2°27′07.4″E	26-Jul	4	4.8	83.8
				28-Jul	6	7.6	99.4
				4-Aug	13	16.9	116
				11-Aug	20	25.6	141.6
				16-Aug	25	32.7	141.8
C	2021	Evasion	Bavinchove	23-Jul	1	0	0
			50°47′11″N	26-Jul	4	4.8	83.8
			2°27′1″E	28-Jul	6	7.6	99.4
				4-Aug	13	16.9	116
				9-Aug	18	23.1	139.8
				16-Aug	25	32.7	141.8
D	2022	Félice	Killem	6-Jul	1	0	0.6
			50°57′04.18″N, 2°34′55.59″E	18-Jul	13	22.6	0.8
				28-Jul	23	42.6	8.2
				8-Aug	34	61.8	10.8
				18-Aug	44	85.8	16.6
				29-Aug	55	105.7	17
				**12-Sep	69	129.4	43.4
				**3-Oct	90	171.9	202.4

* Cumulative days correspond to the number of days between the uprooting of flax and harvesting of retted straw for scutching.
** Extra retting days correspond to sampling points collected on the field after the farmer harvested the flax straw for scutching.

through score plots, loadings, and variable importance plots, while confusion matrices and ROC curves were generated using *caret* and *pROC* (v.1.18.5) R packages. For the confusion matrix, three biological replicates were randomly selected from each dataset where more than three were available to ensure data uniformity. The statistical models were trained using data from three fields and tested using data from the fourth field, so that the training data and test data were independent. Predicted class labels were compared to the actual labels using a confusion matrix, which summarized correct classifications (True Positives) and misclassifications (False Positives and False Negatives). From this, sensitivity and specificity were calculated for each class to evaluate the model's classification performance. Sensitivity (or True Positive Rate) is the proportion of actual positive cases that are correctly identified as positive, whereas specificity assesses the model's ability to correctly exclude other classes—such as avoiding mislabelling advanced-stage samples as beginning-stage (Florkowski, 2008). These metrics were used to generate ROC curves, where the Y-axis represents sensitivity and the X-axis represents specificity.

3. Results

3.1. Field retting dynamics

Retting was monitored for four fields across three different years (field A in 2014, fields B and C in 2021, and field D in 2022) and spectral colorimetric data were acquired to generate four datasets named A to D respectively (Table 1 and **Supplementary Table 1**). The end of retting process was determined by the expertise of farmers, who decided to collect the straw from the field after 44 days of retting in 2014 (Field A), 25 days in 2021 (for Field B and C), and 55 days in 2022 (for Field D). During each retting period, temperature and rainfall data were collected and then cumulative rainfall and cumulative normalized days ND15 were calculated (**Supplementary Data 3**). Cumulative ND15 at retting completion reached 55.76 for field A, 32.78 for field B and C, and 105.76 for field D, while cumulative precipitation totalled 175.4 mm, 141.8 mm and 17 mm, respectively (Table 1). Field A (2014) and fields B and C (2021) show similarly gradual increases in cumulative ND15 up to the end of retting. In contrast, field D (2022) shows a much faster accumulation of ND15, becoming clearly distinct from the other fields during the retting period. This accumulation continues to increase steeply during the additional retting days, 69 and 90 (**Supplementary Data 3**).

3.2. Clustering analysis of flax stem visible spectral datasets

To examine the colour changes during the flax retting process, a spectral database was acquired over a period of three years on four different fields (**Supplementary Table 1**, **Supplementary Data 1a**). K-means clustering was performed on the normalized values of each dataset individually (Fig. 2, **Supplementary Fig. 5**, **Supplementary Data 4**). In datasets A, B, and C, K-means consistently identified four distinct clusters (Fig. 2**(a), (b) and (c)**). In contrast, six clusters were identified in dataset D (Fig. 2**(d)**). In all cases, the clustering forms, group of data from specific retting days or combinations of multiple days. Nonetheless, in the 2022 dataset (Dataset D), four of the clusters were analogous to those observed in the other datasets, while a fifth cluster (named cluster 5 on Fig. 2) was uniquely associated with an extended retting point (day 90). The sixth cluster (named cluster 6 on Fig. 2) comprised data points from various days, which were categorized as outliers or atypical values. This can be due to biological heterogeneity profoundly seen in case of prolonged retting (unfavourable weather). Despite differences in retting years and field locations, the clusters reveal consistent patterns of retting across all four datasets, allowing the consolidation of the data into four distinct retting stages—beginning, early, middle, and advanced— (Table 2). Extra retting points measured in 2022 were split between a new cluster (day 90) and advanced stage (day 69) (Fig. 2**(d)**). These extra points will be considered separately during future analysis.

3.3. Flax stems colour changes during dew retting within the CIE Lab colour space

Visual assessment of flax stems during retting revealed a progressive

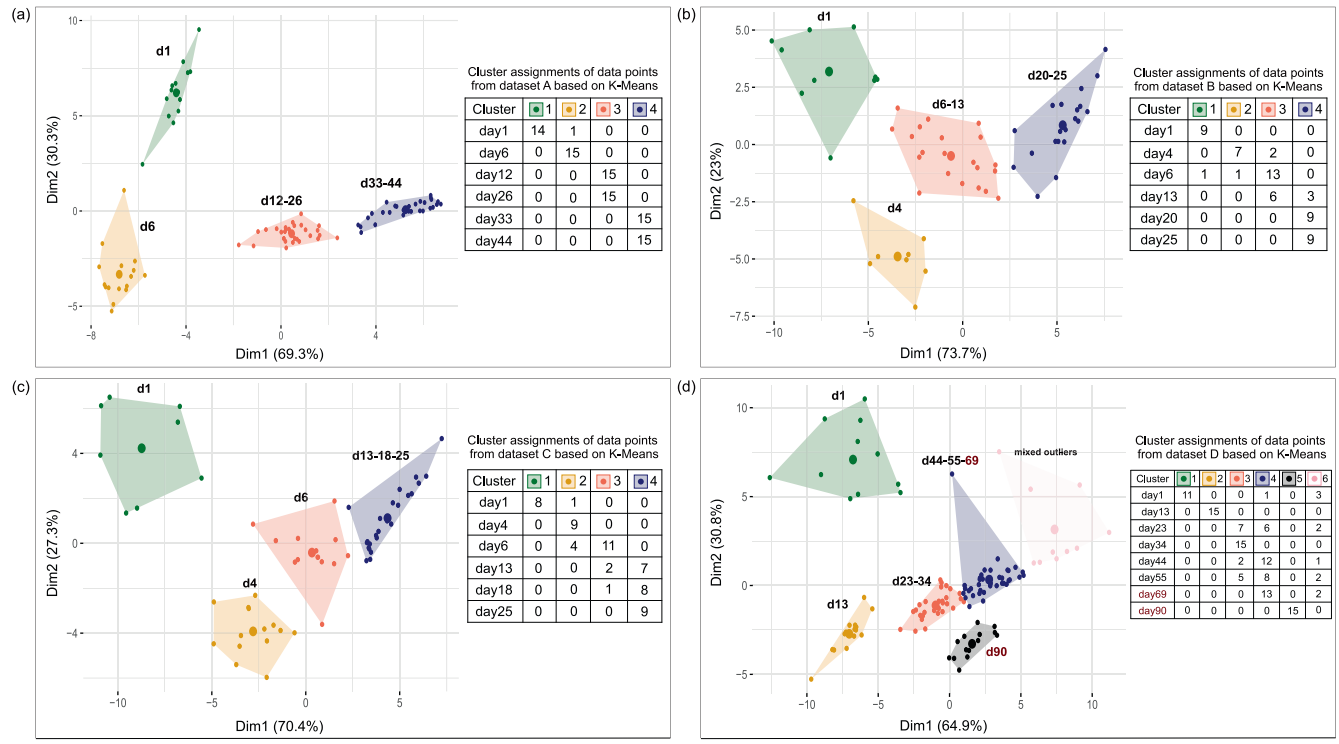

Fig. 2. Clustering of retting days by the K-means method (Supplementary Data 4). The representation of clusters based on stem surface colour reflectance during retting is illustrated in figures a, b, c, and d, corresponding to the dataset A, B, C, and D, respectively. Tables in each figure part show sample numbers assigned to clusters.

Table 2
Relative retting stages based on the time points grouping.

Datasets	Retting time points (days) grouping in stages				Extra-points
	Beginning (Beg.)	Early (Ear.)	Middle (Mid.)	Advanced (Adv.)	
A	1	6	12, 26	33, 44	–
B	1	4	6, 13	20, 25	–
C	1	4	6	13, 18, 25	–
D	1	13	23, 34	44, 55	69, 90

colour transition from green-yellow in the early stages to grey in the middle stages, and to blue-grey in advanced stages. Over-retted stems displayed dark brown to black colouration (**Supplementary Fig. 4**). We quantified these colour changes using the CIE Lab colour system (**Supplementary Data 5**), which is widely used in research and industry. Across all four retting data sets collected over three years, the b* values exhibited a more than 50 % reduction between the beginning and the advanced stages of retting (Fig. 3), following a gradual trend. The a* values increased during early retting stages (Beg. to Ear.) and then decreased towards the later stages, showing a modest overall variation. Changes in L* values were more pronounced in longer retting durations, such as in the dataset A (2014) and D (2022), than in shorter durations like that of B and C (2021) (Fig. 3). In the extra-retting time points, b* and L* values continued to decrease, while a* values increased.

3.4. Multivariate analysis of flax stem visible spectral datasets

To address the complexity of the acquired colour data, in which each wavelength acted as a variable with respect to retting time, multivariate analyses were conducted. Normalized spectral data were first subjected to unsupervised Principal Component Analysis (PCA) for each retting dataset individually. The number of principal components (PCs) was determined using 'scree plots'. In all datasets, scree plots (Fig. 4**(a)**, **Supplementary Fig. 6(a), 7(a), 8(a)**) reveal that the first two components (PC1 and PC2) consistently captured over 90 % of the variability, enabling clear visualization and interpretation of spectral differences among samples. For instance, in dataset A (44-day retting period), the PC1 and PC2 together explained more than 95 % of the variance (Fig. 4 **(a)**).

Subsequently, supervised Partial Least Squares Discriminant Analysis (PLS-DA) confirmed that X-variate 1 and X-variate 2 effectively differentiated the stages of colour change during retting (Fig. 4**(b)**). In dataset A, the beginning stage (day 1) was predominantly explained by X-variate 2, accounting for 30 % of the variance. The early (day 6), middle (days 12–26), and advanced stages (from day 33 onwards) were primarily associated with X-variate 1, which explained 69 % of the variance.

Component loading plots (Fig. 4**(c)**) for X-variates 1 and 2 identified specific wavelengths contributing to retting-stage differentiation. Positive and negative loadings reflected correlations between specific wavelengths and retting time points. Heatmaps or Clustered Image Maps (CIMs) based on X-variates 1 and 2 further resolved distinct spectral patterns across stages (Fig. 5). In dataset A, the beginning stage (day 1) was characterized by strong positive contributions (>1.6, colour scale) from wavelengths in the 510–630 nm range (green, yellow, orange). By early stage (day 6), spectral contributions shifted to the 610–700 nm range. During the middle stage (days 12–26), contributions across the 400–700 nm spectrum remained uniformly low. In the advanced stage (days 33 and 45), spectral contributions were segmented into three distinct blocks: (i) very low (560–660 nm and 690–700 nm; 0 to –3.2), (ii) low (670–680 nm; ≥0), and (iii) high (400–530 nm; 0 to + 3.2) on the colour scale.

Similar patterns were observed in the remaining datasets. In the 2021 datasets B and C (25-day retting period), PLS-DA results showed that the beginning stage (day 1) was explained by X-variate 2, accounting for 23 % (B) and 27 % (C) of the variance, while the early (day 4), middle (days 6–13 in B, day 6 in C), and advanced (days 20–25 in B,

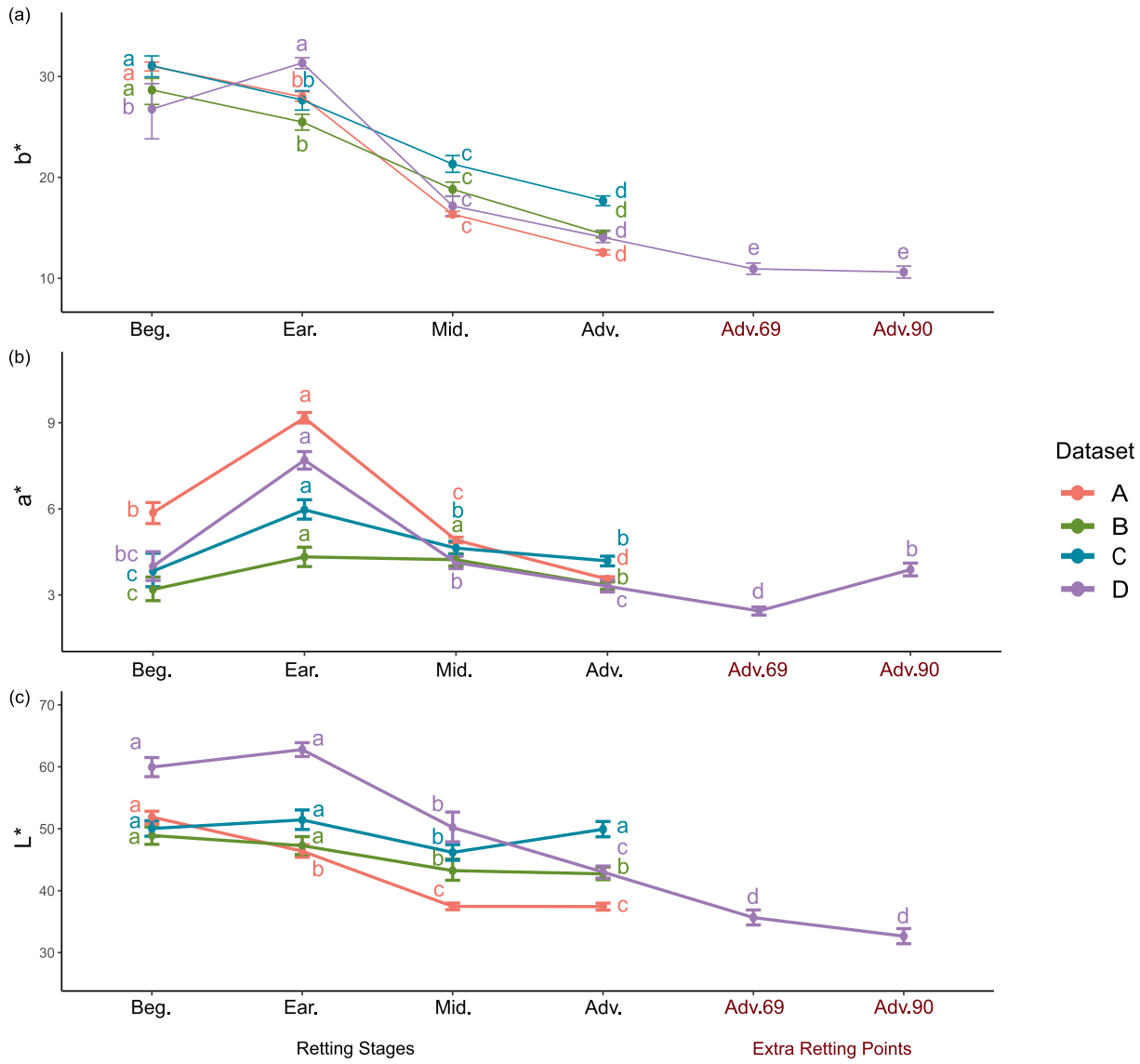

Fig. 3. CIE L*a*b* values of stem surface colour compared between datasets (fields) in relative retting groups and extra retting points (Supplementary Data 5). Figure a, b and c represent b*, a* and L* values respectively, where b* indicates blue-yellowness, a* indicates green-redness and L* shows lightness. Retting stages: Beg. = beginning, Ear. = early, Mid. = middle, Adv. = advanced. The letters represent statistical significance between days (ANOVA, Tukey's HSD test, $P \leq 0.05$).

day 13, 18–25 in C) stages were associated with X-variate 1, explaining 74 % (B) and 70 % (C) of the variance (**Supplementary Fig. 6(b, c), 7 (b, c)**). CIM analysis of dataset B revealed that the beginning stage (day 1) exhibited positive values at 520–630 nm and 690–700 nm (green, yellow, orange). By day 4, the early stage showed increased contributions at 650–680 nm (red). During the middle stage (days 6–13), spectral contributions remained low across the entire 400–700 nm range. In the advanced stage (days 20–25), spectral patterns were again divided into three blocks: (i) very low (520–640 nm and 690–700 nm; 0 to –2.74), (ii) low (650–680 nm; ≥0), and (iii) high (400–510 nm; 0 to + 2.74), corresponding to violet-blue regions (Supplementary Fig. 6(**d**)). Similar clustering and colour-shift patterns were observed in dataset C (**Supplementary Fig. 7(d)**).

In the 2022, dataset D (55-day retting period), a consistent stage-specific colour trend was identified through both PLS-DA and CIM analysis (**Supplementary Fig. 8**). X-variate 1 explained 65 % and X-variate 2 explained 33 % of the variance. The beginning stage (day 1) showed high positive values in the 520–630 nm and 700 nm range (green, yellow, orange). By day 13 (end of early stage), an increase in contributions at 640–690 nm was observed. During the middle stage (days 23–34), colour values across the spectrum remained consistently low. In the advanced stage (days 45–55), typical patterns were observed with increased contributions in the 400–510 nm range (violet-blue), very low values in the 530–630 nm and 690–700 nm range (0 to –3.23), and low contributions in the 650–680 nm range (≥0), thereby recapitulating the colour shift trends observed in the previous datasets.

The loading values of the first X-variate (X-variate 1), which accounts for 65–74 % of the total covariance across all four datasets, are presented in Table 3 along with their corresponding variable weights (**Supplementary Data 6**). The two variables with the highest positive (600, 610 nm) and the two with the highest negative (480, 490 nm) average loading weights were identified.

3.5. Testing of selected wavelengths (480, 490, 600 and 610) for flax retting stage prediction

Multivariate classification models were trained using a matrix (**supplementary data 7**), grouping a subset of three fields, which enabled it to learn to distinguish between classes (Beg., Ear., Mid., Adv.) based on measured input features on selected wavelength variables

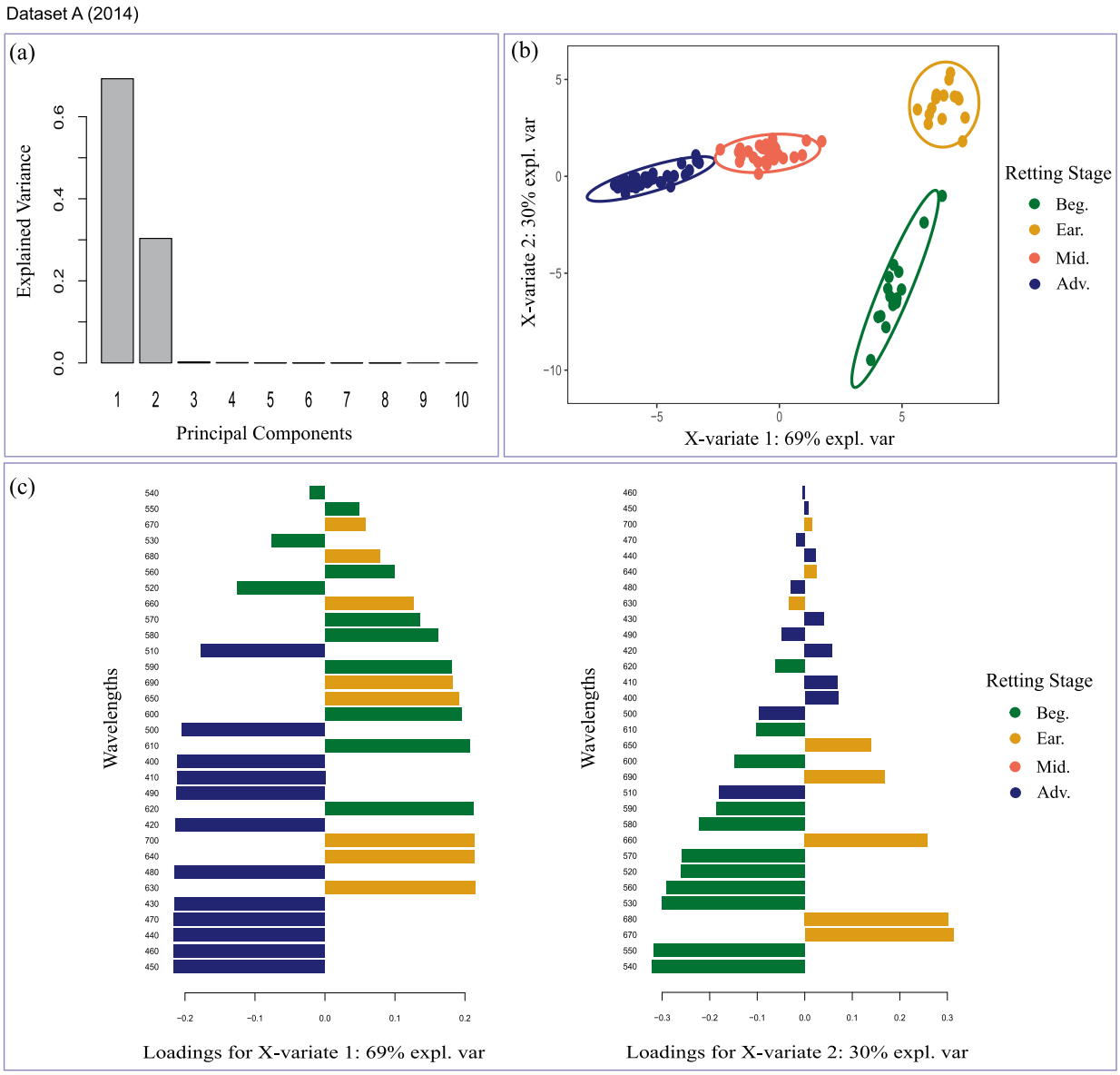

Fig. 4. Multivariate analysis of spectral data of Dataset A (Supplementary Data 1, 2 and 6). (a) Scree Plot of first ten principal components of PCA showing the amount of explained variance; (b) dot plot of samples projected into the X-variate space (after PLS-DA), samples are coloured according to the retting stages defined in Table 2. X-variate 1 explains 69 %, and X-variate 2 explains 30 % of the variance in the data variables; (c) loading plots of X-variate 1 and 2. Colours indicate the retting stages (Beg. = beginning, Ear. = early, Mid. = middle and Adv. = advanced). The scale bar indicates the weight of each variable to the corresponding X-variate.

(480, 490, 600, and 610) (Szymańska et al., 2012). Each model was then tested on the fourth field dataset. In the graph presented in Fig. 6**(a), 6 (d)**, specificity starts at 1, representing perfect classification with no false positives, and decreases toward 0 as the false positives begin to occur (Fig. 6**(c), Supplementary Fig. 9**). The Area Under the Curve (AUC) for each ROC plot quantifies the model's overall ability to distinguish between classes.

Training the model using datasets B, C, and D, and testing it on dataset A yielded strong AUC-ROC values ranging from 0.97 to 1, demonstrating the model's robustness in distinguishing beginning, early, and advanced retting stages (Fig. 6**(a), (d)**). Similar performance was observed when other datasets were used for testing, confirming both the model's consistency and the reproducible nature of retting-associated colour changes over different years (**Supplementary Fig. 9**, **Supplementary Table 2**).

We also build linear classifiers for each of the considered retting stages (**Supplementary Data 8**). Linear classifiers allowed us to calculate ratings of the retting stages which were transformed to the retting stage probability. The model, which had 13 predictors, correctly classified retting stages like beginning, early, middle and advanced, 86 % of the time (**Supplementary Data 9**). Two variables from thirteen were most informative in the classification models: SCI of 490 and 600 nm. Bivariable model for four class (beginning, early, middle and advanced) classification gave 77 % of right classification on a validation dataset (**Supplementary Data 9**).

3.6. *Characterization of over-retting points*

The additional retting time points (d69 and d90) from the Dataset D samples (retting 2022) were analysed along with the last retting time point of the advanced stage (d55) to determine whether extra-retting can be distinguished based on colorimetric parameters. PCA showed

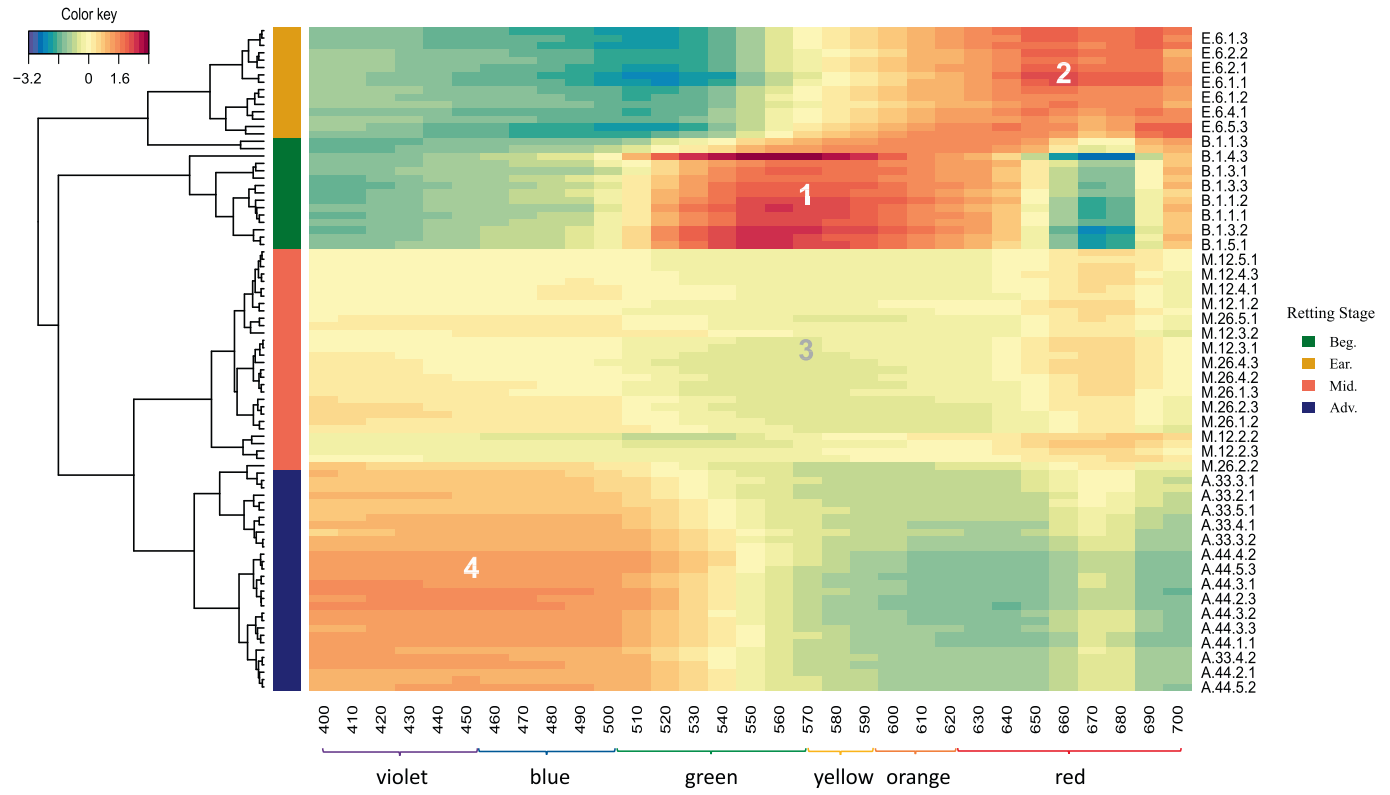

Fig. 5. The heatmap of respective PLS-DA loading weights of wave-length variables (Dataset A). Colour scale represents the loading weights of respective variables. On the left side of the heatmap, individual samples names are encoded as X.Y.Z.K where X represents Relative groups, Y represents day of sampling, Z represents Replicate number, K represents the position of measurement along the flax stem (bottom = 1, middle = 2 and top = 3).

Table 3
Summary of PLS-DA loading values from X to variate 1 (explaining 65–74% of covariance) for dataset A-D, highlighting wavelengths with the highest and lowest average loadings. Full table in Supplementary data 6.

Wavelengths	Comp1 Loadings Dataset A	Comp1 Loadings Dataset B	Comp1 Loadings Dataset C	Comp1 Loadings Dataset D	Average Loading ± SD
480	−0.214484427	−0.2039411	−0.208338215	−0.20182853	−0.207148068 ± 0.005
490	−0.212426754	−0.203853267	−0.208704063	−0.203982974	−0.207241764 ± 0.004
….					
600	0.194851123	0.210820797	0.213832036	0.24700028	0.216626059 ± 0.02
610	0.206585489	0.209678795	0.206770846	0.244134064	0.216792299 ± 0.018
…					

that the first two components accounted for the majority of the variability in the dataset (Fig. 7 **(a)**). PLS-DA revealed that X-variate 1 explained 55 % of the covariance, clearly separating d90 from overlapping d55 and d69 (Fig. 7**(b)**). In contrast, X-variate 2, which explained 44 % of the covariance, demonstrated potential for separating d55 from both d69 and d90. Analysis of loading weights on X-variate 1 indicated that the 510–590 nm wavelength range (green-yellow) was associated with d55 and d69, whereas the 660–700 nm range (red) was characteristic of d90 (Fig. 7**(c)**). For X-variate 2, the 580–620 nm range (yellow-orange) was associated with d55, while the 400–470 nm range (violet-blue) defined d69.

4. Discussions

4.1. Empirical flax dew-retting and colour changes

Visual observations of the flax retting process done within this study was in accordance with what has already been observed in previous studies on hemp (Bleuze et al., 2018; Mazian et al., 2019; Bou Orm et al., 2024). For example, during hemp dew retting, it has been shown that stem samples initially present a vivid green colour, which turns bright yellow within the first week. By the second week, black spots begin to appear, and by the fourth week, the appearance shifts to pale grey with additional black spots. Finally, by the sixth week, the stems become dark grey with numerous black spots. These colour changes during dew retting might result from a mix of biological and chemical processes: degradation of plant pigments, oxidation, biodegradation, and microbial colonization (Lee and Gould, 2002; Sousa, 2022; Lu et al., 2023). First of all, chlorophyll, the pigment that gives plants their green aspect, breaks down (releasing the pyrrole rings) as a plant goes into senescence and finally dies, causing a noticeable change to yellow, orange, or brown. Enzymatic processes and environmental constraints such as UV exposure cause oxidation which turns chlorophyll into non-coloured molecules and makes other pigments like carotenoids more visible (Hu et al., 2021; Sousa, 2022). Some proteins related to protection during UV stress such as UvrA or UrvC proteins were revealed in flax retting metaproteome (Mukherjee et al., 2024). Retting results from microbial actions and could speed up these modifications. The emergence of black spots can be linked to microbial activity, as noted in previous hemp studies (Jankauskienė and Gruzdevienė, 2013; Bleuze et al., 2018; Bleuze et al.,

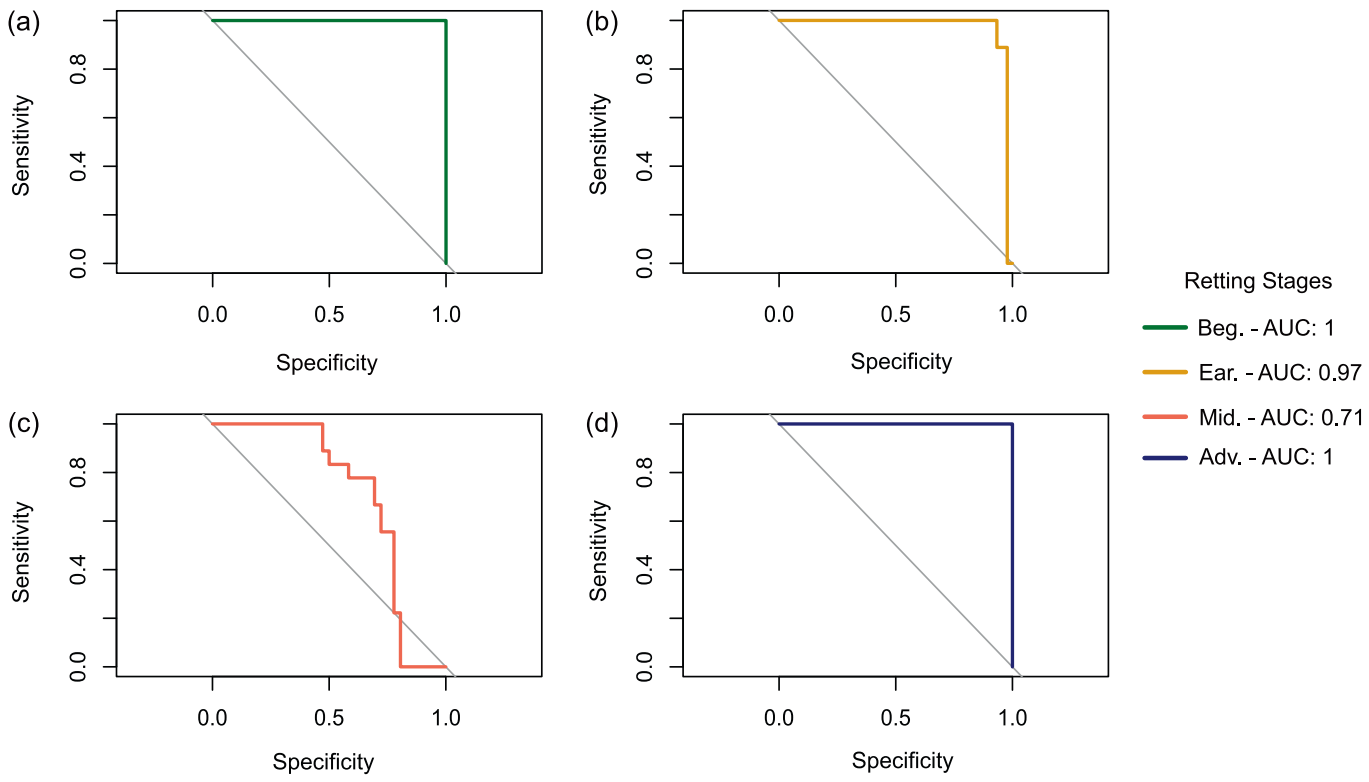

Fig. 6. Testing statistical predictive model built with data from datasets B to C, with data from Dataset A. ROC curves with Area under the curve (AUC) score of (a) Beg. = beginning retting stage, (b) Ear. = early retting stage, (c) Mid. = middle stage of retting and (d) Adv. = advanced retting stage from dataset A (retting 2014) with prediction model trained from pooled data including values from datasets B, C and D (supplementary Data 7 and 10). (AUC score of 1 indicates perfect performance of prediction and 0.5 indicates random assignment).

2020). Phenolics could be released when bacteria and fungi break down structural elements such as lignin, further oxidizing and darkening the surface of the stem (Chowdhary et al., 2021). Reactive oxygen species produced during this breakdown add to oxidative browning, which intensifies the darkening over time (Hu et al., 2021). Moreover, fungi or bacteria might contribute to colour changes by producing pigments, such as melanin (Eisenman and Casadevall, 2012). *Aspergillus* spp. known to produce melanin (Suthar et al., 2023) have been identified during retting in previous studies of both flax (Fila et al., 2001; Djemiel et al., 2020) and hemp (Nykter et al., 2008; Bou Orm et al, 2025). These interplaying biological and chemical processes can explain the gradual colour change in the stems of retted plants but certainly need to be studied in the context of flax retting.

Since visible colour changes result from a series of complex transformations of the stem (biological and chemical), simple perception cannot capture their full extent. Moreover, as the colour of the stems may not be completely uniform, measuring colour changes using a spectro-colorimeter may show some variability. However, most devices calculate the average colour values over a defined surface area (8 mm medium measurement aperture in the case of the CM-23d, Konica Minolta), and several measurements are generally necessary- both at different points along the stem and across several batches of stems.

4.2. *The K-means clusters of spectral datasets define a pattern of retting*

Different weather conditions, soil composition and other environmental factors such as rainfall, temperature, exposure to sunlight (radiations) *etc.* might affect the biology of the retting process of flax (Martin et al., 2013; Djemiel et al., 2017; Chabbert et al., 2020) and other fibre plants (Chabbert et al., 2023; Bou Orm et al., 2024). Variations in these parameters were clearly observed across the years and fields considered in this study. For example, soil analysis shows a notable difference in clay content between field A (15 %) and fields B and C (26 to 31 %). This indicates that the 2021 fields might have a greater water retention capacity, which could explain the shorter retting during observed in fields B and C in 2021 (25 days), as compared to field A in 2014 (44 days), with more or less comparable meteorology (**Supplementary Figs. 1, 2**). Carbon content of Field B and C are higher than Field A, but the C/N ratio that drives the microbial activity are quite similar (**Supplementary Fig. 2**). Moreover, the overall composition of flax stems themself (and particularly C/N ratio), depending mainly on culture conditions, might also influence the priming of material degradation (Liang et al, 2017). Climate parameters might also explain different retting duration and dynamic, which can last four weeks, as in 2014, or eight weeks, as in 2022 (Table 1). Retting progressed over roughly 30 to 60 cumulative ND15 for field A (55.76) and fields B and C (32.78), which aligns with the range observed in hemp retting studies by Chabbert et al., 2023. By contrast, Field D required 105.76 cumulative ND15, well above this suggested range. This might be explained mainly by the water deficit received by this field (17 mm of cumulative rains) compared to others (175.4 mm in field A and 141.8 mm in fields B and C) (**Supplementary Fig. 1, Supplementary Data 3**). Experts agree on the need for water for retting to progress (Martin et al., 2013), and periods of low rainfall can greatly delay the process. Cumulative ND15 and cumulative rainfall capture the effects of temperature and moisture on retting, yet such variability makes direct time-based comparisons across multiple years unreliable. Because retting is influenced by both environmental and biological factors. To address this, we applied K-means clustering of stem colour/ spectral data to define relative retting stages. This approach is well supported, as colour changes (spectral signatures) are widely used proxies for retting progression, and clustering provides a recognized method to standardize comparisons across variable conditions. Stage-based comparisons are therefore more meaningful than absolute time. Initial clustering of the four datasets revealed that,

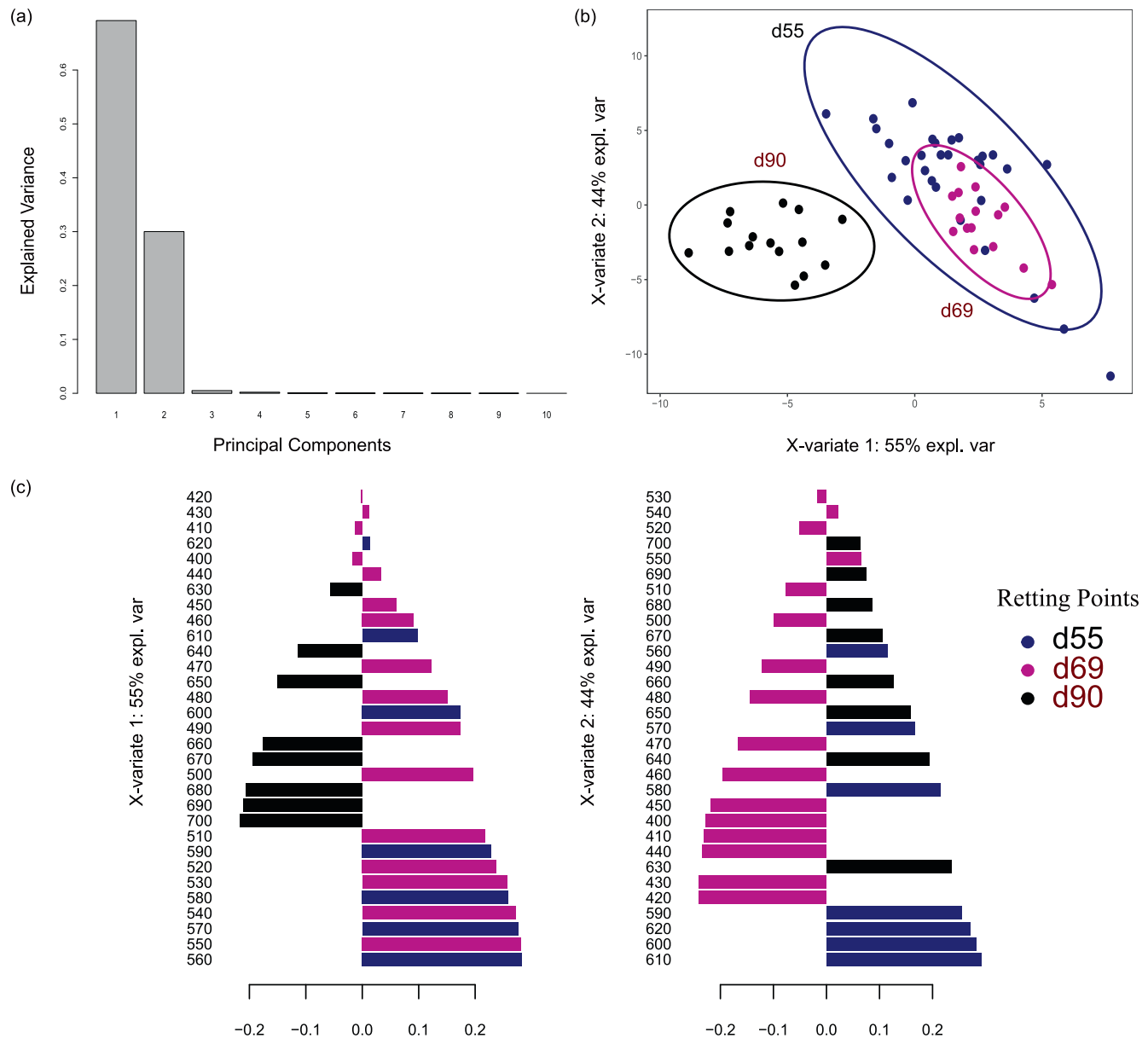

Fig. 7. Multivariate analysis of Dataset D (Supplementary Data 1, 2 and 6) focusing on advanced stages and extra retting points. (a) Scree Plot of first ten principal components of PCA showing the amount of explained variance; (b) dot plot of samples projected into the X-variate space (after PLS-DA), samples are coloured according to the retting stages defined in Table 2. X-variate 1 explains 55%, and X-variate 2 explains 44% of the variance in the data variables; (c) loading plots of X-variate 1 and X-variate 2. Colour indicates the retting points (d55, d69 and d90). The scale bar indicates the weight of each variable to the corresponding X-variate.

despite variations in retting duration across different years, the process follows a consistent sequence of spectral changes, allowing samples to be grouped into common retting stages (beginning, early, middle, and advanced). While a direct link between these stages and cumulative ND15 is not obvious, we can suggest that retting end point may correspond to a cumulative ND15 of roughly between 30 and 60, provided cumulative precipitation reaches more than 140 mm or at least about 50 mm but with prolonged retting duration how it was the case of field D (**Supplementary Fig. 1**). Comparable values of cumulative ND15 and precipitation were observed in hemp retting studies (Chabbert et al., 2023). Nonetheless, the stage distinctions obtained by K-means clustering seem to correspond with known enzymatic, microbial, and biochemical patterns of dew retting described in previous studies. For example, Mukherjee et al, 2024 described the following: beginning/ early stages are marked by peroxidase and phenoloxidase activity, early/ middle stages by polygalacturonase, middle stages by increased activities of xylosidase, galactosidase, cellobiohydrolase, and advanced by cellulase and glucosidase.

4.3. CIE Lab evaluation of flax stem colour dynamics during retting

By instrumental measurement, we captured surface light reflectance across the visual spectrum and expressed them in the CIE Lab colour space. This system uses three values to represent colour, i.e. blue/yellow (b*), green/red (a*) and lightness (L*). Colour differences in Lab space closely match human perception and ensure consistent representation across devices (Fairchild, 2013). The CIE Lab colour space is commonly used and measured by industrial spectro-colorimeters. Some of them used this approach to characterize and classify already retted extracted fibres batches from flax (Akin et al., 2000; Peyrache et al., 2024). Previous studies have already reported the CIE Lab colour space for the hemp retting (Bleuze et al., 2018). Other studies have shown the value of spectral analysis in assessing physiological processes in plants, such as fruit ripening (Merzlyak et al., 2003). Our study observed the a* and b*

values decreased by over 50 % from the start to the end of retting, reflecting a significant shift in colour metrics. This reduction corresponds to a shift from green to achromatic grey tones. While the L* value exhibited a general downward trend, this pattern varied across the three years of samples, reflecting a transition from brightness to darker shades (Fig. 3). Obtained data are consistent with prior findings on hemp. CIE Lab colour analysis of hemp stems during retting further highlights decreases of a* (red-green axe) and b* (yellow-blue axe) values by 32.2 % and 32.4 %, respectively, approaching zero. Concurrently, the L* value, representing lightness, decreases by 18.5 % (Bleuze et al., 2018). The CIE Lab values for extra-retted flax samples display the lowest L* value, indicating a duller and darker appearance, along with the lowest a* and b* values, which further represent this bluish shift. However, CIE Lab is not precise enough to detect subtle colour changes because it can show significant deviations from actual perception, especially in certain regions of colour space (Sharma and Rodríguez-Pardo, 2012; Seymour, 2022). Multivariate analysis using the full visible spectrum would be a more efficient approach to capture these subtle and complex changes, and so far, build an infield tool that can monitor the dew retting.

4.4. Multivariate analysis of colour patterns to identify key retting wavelengths

Multivariate statistical analyses—particularly PCA and PLS-DA—further confirmed these shared progression patterns and led to the identification of key wavelength variables that can be used to discriminate these stages. This tends to show that, regardless of duration, year, or local conditions, retting seems to follow a broadly universal process. This has also been shown from a biological point of view during the enzymatic characterisation of the process in the course of other studies in flax (Chabbert et al., 2020; Mukherjee et al., 2024).

In our study, PLS-DA proved especially valuable as both a feature selector and a classifier, enabling effective differentiation of retting stages based on spectral data. This approach has been firstly applied to Raman spectral data in stressed flax (Blervacq et al., 2023), or FT-IR spectral data during flax dew retting (Mukherjee et al., 2025). Although limitations have been noted when class separation relies on complex linear or nonlinear relationships (Ruiz-Perez et al., 2020), PLS-DA performs robustly in scenarios like ours where classes exhibit clear clustering based on spectral features. The continuous and collinear structure of spectral data makes linear methods such as PCA and supervised PLS-DA particularly suitable, as they reduce noise, handle collinearity, and extract interpretable components for regression, classification, and biomarker discovery (Gu et al., 2011). Thus, PLS-DA was preferred to other non-linear methods like t-SNE and UMAP. The latter are better suited for datasets such as omics data, where capturing local neighbourhood structures and revealing subtle subpopulations is the primary objective (Xia et al., 2024; Jeon et al., 2025). In the context of retting, PLS-DA loadings revealed a reproducible shift in dominant wavelength contributions over time. Initially, spectral variables between 520–630 nm were most influential, indicating a green-yellow to orange colouration characteristic of freshly harvested flax stems. This was followed by increased contributions from the 650–680 nm range, suggesting an orange-red transition as retting progressed. In later stages, a marked shift occurred: variables in the 400–510 nm range gained prominence, corresponding to a violet-blue hue, while contributions from the red region (650–680 nm) diminished, and the initial green-yellow-orange tones were no longer present (Fig. 5**, Supplementary Fig. 6(d), 7(d), 8(d)**).

More specifically, analysis of the first latent variable (X-variate 1) across all datasets revealed a consistent trend: reflectance values at 480 and 490 nm increased, while values at 600 and 610 nm decreased from the beginning to the advanced stages of retting. This spectral evolution suggests a progressive colour shift from orange to blue on the stem surface, which corresponds well with the visual changes we observed on the field during retting (**Supplementary Fig. 4**).

To evaluate whether a reduced set of wavelengths could suffice for stage discrimination, we tested classification performance using selected spectral bands (*e.g.,* 480, 490, 600, 610 nm) via confusion matrix analysis and ROC AUC curves (Fig. 6**, Supplementary Fig. 9**). Results from these metrics confirmed that a reduced subset of wavelengths is indeed capable of distinguishing between retting stages with high accuracy, demonstrating the feasibility of simplified, targeted spectral monitoring for process control.

Since absorbance values at wavelengths only 10 nm apart (*e.g.*, 480–490 nm and 600–610 nm) may be correlated, there could be a risk of overfitting when training the model. However, a bivariable model using only 490 nm and 600 nm absorbance achieved comparable classification accuracies—66.7 % for the beginning stage, 77.8 % for the early stage, 78.6 % for the middle stage, and 80.0 % for the advanced stage—on the validation dataset (calculated according to **Supplementary. Data 9**). Comparable model performance implies that overfitting is unlikely with four variables, which are preferred to avoid losing critical information for accurately monitoring retting.

Taken together, these findings underscore the advantage of full-spectrum multivariate analysis over traditional colour spaces such as CIE Lab and highlight its potential to select wavelength for monitoring in real-time and in a non-invasive way the retting progression. As a next step towards optimization, it will be essential to assess instrumental in-field colour perception under different weather conditions and evaluate the robustness of the model developed from laboratory-obtained data. Additionally, exploring wavelengths beyond the visible range such as ultraviolet or near-infrared regions to capture deeper chemical and structural changes, as seen in case of Salix clones' chemical properties (Bouaziz et al., 2025), which might be a way to add other markers in the model, such as biological (Mukherjee et al., 2024) or chemical (Chabbert et al., 2020; Mukherjee et al., 2025).

4.5. Discrimination of under or over dew-retting point

The advanced retting stage corresponds to the endpoint set by experienced farmers' field observations. What happens after this optimal point (over-retting) is unclear, so dataset D adds two later samplings (days 69 and 90, beyond the day-55 endpoint) to track surface colour changes during extended retting.

PLS-DA analysis demonstrated that the first latent variable (X1) effectively separated day 90 from days 55 and 69 (Fig. 7). Day 90 exhibited high loading contributions in the 660–700 nm range, indicative of a red-shifted surface colour, whereas both day 55 and day 69 showed dominant contributions in the 510–590 nm region, corresponding to green-yellow hues. This spectral distinction suggests that day 90 represents a more advanced stage of retting compared to the earlier time points.

Furthermore, the second latent variable (X2) provided additional resolution, revealing that day 55 was primarily associated with wavelengths between 580–620 nm (yellow-green), while day 69 shifted toward the 400–460 nm range, characteristic of violet-blue tones. This shift implies continued colour transformation beyond the conventionally defined endpoint, highlighting that retting may still be progressing chemically and visually. By the time flax was harvested from the field in 2022 (dataset D), the degree of retting might not be optimal, but the organizational conditions of agricultural work imposed a limitation on the duration of this process (personal communication from farmers). It can be assumed that due to the low cumulative precipitation, the physical and chemical components of the flax retting process prevailed over the biological ones for a long time. We assume, because of the actual lack of water at the beginning stage of retting, a microbial community might not develop as fast as in field A, B and C, and enzymatic reactions might be slowed down. This greatly increased the duration of retting in the field D, and the day 69 samples which were collected after the official end of the retting process, demonstrated the continuing dynamics of the process. Meanwhile, the day 90 samples showed

differences in spectral characteristics and were over-retted samples.

5. Conclusions

In this study, we explored the evolution of flax stem surface colour during dew retting by acquiring visible spectral reflectance, which is an objective measurement of colour changes. Using a portable commercial spectrophotometer, we successfully recorded colour changes both in CIE Lab space colour and visible spectra from 400 to 700 nm, in three different retting years (involving four flax fields). Due to the development of an original multivariate statistical pipeline based on unsupervised (PCA) and supervised (PLSDA) methods, we identified four wavelengths (480, 490, 600, and 610 nm) as reliable markers of retting progression observed in four independent retting process. Based on these wavelengths, a statistical model was built and showed efficiency to predict the retting stage with a high degree of confidence. This work has proved the concept that, by using a simple measurement that can be easily automated and implemented by the use of drones and tuning them to measure colour from a distance, it is possible to monitor the progress of retting reliably. Further future in situ retting studies will help generate data to enhance the model's reliability and field applicability. Potentially, this approach could be applied to other crop species that require field retting for their processing (*e.g.*, hemp). This opens the door to the development of digital tools which, coupled with artificial intelligence (and other retting markers), will help farmers to determine the best time to stop retting, thereby increasing fibre quality, yield, and batch homogeneity and thus bring flax growing into the era of Agriculture 4.0.

Fundings

This work was performed within the framework of the PEARL Flax-Tronic project co-funded by the European Union's Horizon 2020 research and innovation program under the Marie Skłodowska-Curie grant agreement N°847568, and the I-SITE ULNE Fondation (ANR), DG was granted by College de France PAUSE program (https://www.college-de-france.fr) and the University of Lille (https://www.univ-lille.fr).

Declaration of Generative AI and AI-assisted technologies in the writing process

Authors did not use generative AI and AI-assisted technologies in the writing process of this manuscript.

CRediT authorship contribution statement

Suvajit Mukherjee: Writing – review & editing, Writing – original draft, Visualization, Methodology, Investigation, Formal analysis, Data curation, Conceptualization. **Dmitry Galinousky:** Writing – review & editing, Visualization, Validation, Investigation, Formal analysis. **Anne-Sophie Blervacq:** Writing – review & editing. **Lionel Buchaillot:** Writing – review & editing, Funding acquisition. **Steve Arscott:** Writing – review & editing. **Sébastien Grec:** Writing – review & editing, Validation, Supervision, Project administration, Methodology, Funding acquisition, Conceptualization.

Declaration of competing interest

The authors declare the following financial interests/personal relationships which may be considered as potential competing interests: Suvajit Mukherjee reports financial support was provided by European Union. Dmitry Galinousky reports financial support was provided by College of France. Suvajit Mukherjee reports financial support was provided by I-SITE ULNE Fondation. If there are other authors, they declare that they have no known competing financial interests or personal relationships that could have appeared to influence the work reported in this paper.

Acknowledgments

Dr. Suvajit Mukherjee would like to thank the I-Site ULNE foundation for funding and M. Alexis Boulet for coordinating the PEARL (Programme for Early-stage Researchers in Lille) program. The authors thank Dr. Ali Reda from IEMN (UMR 8520), and Dr. Christophe Djemiel for their valuable help in collecting samples. Our industrial partners Van Robaeys Frères, F-59122 Killem, are thanked for making the flax fields B, C and D available to us and for carrying out the industrial characterization of flax fibres, as well as the C.A.L.I.R.A (Coopérative Agricole linière de la région d'Abbeville" F- 80140 Martainneville) for making their flax fields available to us.

Ethical approval

We confirm that all the research meets ethical guidelines and adheres to the legal requirements of the study country. The research does not involve any human or animal welfare related issues.

Appendix A. Supplementary material

Supplementary Tables and Figures and Supplementary data to this article can be found online at https://doi.org/10.1016/j.compag.2026.111407.

Data availability

Original data are provided as Supplementary material (Supplementary Data)

References

Akin, D.E., 2013. Linen Most Useful: Perspectives on Structure, Chemistry, and Enzymes for Retting Flax. ISRN Biotechnol. 2013, 1–23. https://doi.org/10.5402/2013/186534.

Akin, D.E., Epps, H.H., Archibald, D.D., Sharma, H.S.S., 2000. Color Measurement of Flax Retted by Various Means. Text. Res. J. 70, 852–858. https://doi.org/10.1177/004051750007001002.

Akin, D.E., Gamble, G.R., Morrison III, W.H., Rigsby, L.L., Dodd, R.B., 1996. Chemical and Structural Analysis of Fibre and Core Tissues from Flax. J. Sci. Food Agric. 72, 155–165. https://doi.org/10.1002/(SICI)1097-0010(199610)72:2<155::AID-JSFA636>3.0.CO;2-X.

Baley, C., 2002. Analysis of the flax fibres tensile behaviour and analysis of the tensile stiffness increase. Compos. A Appl. Sci. Manuf. 33, 939–948. https://doi.org/10.1016/S1359-835X(02)00040-4.

Blervacq, A.-S., Moreau, M., Duputié, A., Hawkins, S., 2023. Comparative Analysis of G-Layers in Bast Fiber and Xylem Cell Walls in Flax using Raman Spectroscopy. Biomolecules 13, 435. https://doi.org/10.3390/biom13030435.

Bleuze, L., Chabbert, B., Lashermes, G., Recous, S., 2020. Hemp harvest time impacts on the dynamics of microbial colonization and hemp stems degradation during dew retting. Ind. Crop Prod. 145, 112122. https://doi.org/10.1016/j.indcrop.2020.112122.

Bleuze, L., Lashermes, G., Alavoine, G., Recous, S., Chabbert, B., 2018. Tracking the dynamics of hemp dew retting under controlled environmental conditions. Ind. Crop Prod. 123, 55–63. https://doi.org/10.1016/j.indcrop.2018.06.054.

Bou Orm, E., Sutton-Charani, N., Bayle, S., Benezet, J.-C., Bergeret, A., Malhautier, L., 2024. Influence of field retting on physicochemical and biological properties of "Futura 75 hemp stems. Ind. Crop Prod. 214, 118487. https://doi.org/10.1016/j.indcrop.2024.118487.

Bou Orm, E., Mukherjee, S., Rifa, E., Créach, A., Grec, S., Bayle, S., Benezet, J.-C., Bergeret, A., Malhautier, L., 2025. Enhancing Biodiversity-Function Relationships in Field Retting: Towards Key Microbial Indicators for Retting Control. Environ. Microbiol. Rep. 17, e70102. https://doi.org/10.1111/1758-2229.70102.

Bouaziz, B., Koubaa, A., Mvolo, C., Koubaa, S., Krygier, R., 2025. Use of NIR spectroscopy and partial least squares regression for prediction of chemical properties of Salix clones. Eur. J. Wood Prod. 83, 176. https://doi.org/10.1007/s00107-025-02320-1.

Bourmaud, A., Siniscalco, D., Foucat, L., Goudenhooft, C., Falourd, X., Pontoire, B., Arnould, O., Beaugrand, J., Baley, C., 2019. Evolution of flax cell wall ultrastructure and mechanical properties during the retting step. Carbohydr. Polym. 206, 48–56. https://doi.org/10.1016/j.carbpol.2018.10.065.

Bratt, R.P., Mercer, P.C., Brown, A.E., 1988. Degradation of flax stems by Botrytis cinerea. Trans. Br. Mycol. Soc. 90, 537–544. https://doi.org/10.1016/S0007-1536(88)80004-4.

Brown, A.E., Sharma, H.S.S., 1984. Production of polysaccharide-degrading enzymes by saprophytic fungi from glyphosate-treated flax and their involvement in retting. Ann. Appl. Biol. 105, 65–74. https://doi.org/10.1111/j.1744-7348.1984.tb02803.x.

Brown, A.E., Sharma, H.S.S., Black, D.L.R., 1986. Relationship between pectin content of stems of flax cultivars, fungal cell wall-degrading enzymes and pre-harvest retting. Ann. Appl. Biol. 109, 345–351. https://doi.org/10.1111/j.1744-7348.1986.tb05326.x.

Chabbert, B., Padovani, J., Djemiel, C., Ossemond, J., Lemaître, A., Yoshinaga, A., Hawkins, S., Grec, S., Beaugrand, J., Kurek, B., 2020. Multimodal assessment of flax dew retting and its functional impact on fibers and natural fiber composites. Ind. Crop Prod. 148, 112255. https://doi.org/10.1016/j.indcrop.2020.112255.

Chabbert, B., Philippe, F., Thiébeau, P., Alavoine, G., Gaudard, F., Pernes, M., Day, A., Kurek, B., Recous, S., 2023. How the interplay between harvest time and climatic conditions drives the dynamics of hemp (*Cannabis sativa L.)* field retting. Ind. Crop Prod. 204, 117294. https://doi.org/10.1016/j.indcrop.2023.117294.

Chand, N., Fahim, M., 2020. Tribology of Natural Fiber Polymer Composites. Woodhead Publishing.

Chowdhary, V., Alooparampil, S., Pandya, R.V., Tank, J.G., 2021. Physiological function of phenolic compounds in plant defense system. Phenolic compounds-chemistry, synthesis, diversity, non-conventional industrial, pharmaceutical and therapeutic applications.

Djemiel, C., Goulas, E., Badalato, N., Chabbert, B., Hawkins, S., Grec, S., 2020. Targeted metagenomics of retting in flax: the beginning of the quest to harness the secret powers of the microbiota. Front. Genet. 11.

Djemiel, C., Grec, S., Hawkins, S., 2017. Characterization of Bacterial and Fungal Community Dynamics by High-Throughput Sequencing (HTS) Metabarcoding during Flax Dew-Retting. Front. Microbiol. 8. https://doi.org/10.3389/fmicb.2017.02052.

Donaghy, J.A., Boomer, J.H., Haylock, R.W., 1992. An assessment of the quality and yield of flax fiber produced by the use of pure bacterial cultures in flax rets. Enzyme Microb. Technol. 14, 131–134. https://doi.org/10.1016/0141-0229(92)90170-S.

Eisenman, H.C., Casadevall, A., 2012. Synthesis and assembly of fungal melanin. Appl. Microbiol. Biotechnol. 93, 931–940. https://doi.org/10.1007/s00253-011-3777-2.

Elfaleh, I., Abbassi, F., Habibi, M., Ahmad, F., Guedri, M., Nasri, M., Garnier, C., 2023. A comprehensive review of natural fibers and their composites: an eco-friendly alternative to conventional materials. Results Eng. 19, 101271. https://doi.org/10.1016/j.rineng.2023.101271.

Fairchild, M.D., 2013. Color appearance models. John Wiley & Sons.

Fila, G., Manici, L.M., Caputo, F., 2001. In vitro evaluation of dew-retting of flax by fungi from southern Europe. Ann. Appl. Biol. 138 (3), 343–351.

Florkowski, C.M., 2008. Sensitivity, Specificity, Receiver-Operating Characteristic (ROC) Curves and Likelihood Ratios: Communicating the Performance of Diagnostic Tests. Clin. Biochem. Rev. 29, S83–S87.

Gomez-Campos, A., Vialle, C., Rouilly, A., Sablayrolles, C., Hamelin, L., 2021. Flax fiber for technical textile: a life cycle inventory. J. Clean. Prod. 281, 125177. https://doi.org/10.1016/j.jclepro.2020.125177.

Gu, H., Pan, Z., Xi, B., Asiago, V., Musselman, B., Raftery, D., 2011. Principal component directed partial least squares analysis for combining nuclear magnetic resonance and mass spectrometry data in metabolomics: Application to the detection of breast cancer. Anal. Chim. Acta 686, 57–63. https://doi.org/10.1016/j.aca.2010.11.040.

Henriksson, G., Akin, D.E., Hanlin, R.T., Rodriguez, C., Archibald, D.D., Rigsby, L.L., Eriksson, K.L., 1997. Identification and retting efficiencies of fungi isolated from dew-retted flax in the United States and europe. Appl. Environ. Microbiol. 63, 3950–3956. https://doi.org/10.1128/aem.63.10.3950-3956.1997.

Hu, X., Gu, T., Khan, I., Zada, A., Jia, T., 2021. Research Progress in the Interconversion, turnover and Degradation of Chlorophyll. Cells 10, 3134. https://doi.org/10.3390/cells10113134.

Jankauskienė, Z., Gruzdevienė, E., 2013. Physical parameters of dew retted and water retted hemp (Cannabis sativa L.) fibres. Zemdirbyste-Agriculture 100, 71–80. https://doi.org/10.13080/z-a.2013.100.010.

Jeon, H., Park, J., Shin, S., Seo, J., 2025. Stop Misusing t-SNE and UMAP for Visual Analytics. Doi: 10.48550/arXiv.2506.08725.

Lee, D.W., Gould, K.S., 2002. Why Leaves turn Red: Pigments called anthocyanins probably protect leaves from light damage by direct shielding and by scavenging free radicals. Am. Sci. 90, 524–531.

Liang, X., Yuan, J., Yang, E., Meng, J., 2017. Responses of soil organic carbon decomposition and microbial community to the addition of plant residues with different C:N ratio. Eur. J. Soil Biol. 82, 50–55. https://doi.org/10.1016/j.ejsobi.2017.08.005.

Lu, X., Li, W., Wang, Q., Wang, J., Qin, S., 2023. Progress on the Extraction, Separation, Biological activity, and delivery of Natural Plant Pigments. Molecules 28, 5364. https://doi.org/10.3390/molecules28145364.

Martin, N., Mouret, N., Davies, P., Baley, C., 2013. Influence of the degree of retting of flax fibers on the tensile properties of single fibers and short fiber/polypropylene composites. Ind. Crop Prod. 49, 755–767. https://doi.org/10.1016/j.indcrop.2013.06.012.

Mazian, B., Cariou, S., Chaignaud, M., Fanlo, J.-L., Fauconnier, M.-L., Bergeret, A., Malhautier, L., 2019. Evolution of temporal dynamic of volatile organic compounds (VOCs) and odors of hemp stem during field retting. Planta 250, 1983–1996. https://doi.org/10.1007/s00425-019-03280-6.

Meijer, W.J.M., Vertregt, N., Rutgers, B., van de Waart, M., 1995. The pectin content as a measure of the retting and rettability of flax. Ind. Crop Prod. 4, 273–284. https://doi.org/10.1016/0926-6690(95)00041-0.

Melelli, A., Shah, D.U., Hapsari, G., Cortopassi, R., Durand, S., Arnould, O., Placet, V., Benazeth, D., Beaugrand, J., Jamme, F., Bourmaud, A., 2021. Lessons on textile history and fibre durability from a 4,000-year-old Egyptian flax yarn. Nat. Plants 7, 1200–1206. https://doi.org/10.1038/s41477-021-00998-8.

Merzlyak, M.N., Gitelson, A.A., Chivkunova, O.B., Solovchenko, A.E., Pogosyan, S.I., 2003. Application of Reflectance Spectroscopy for Analysis of Higher Plant Pigments. Russ. J. Plant Physiol. 50, 704–710. https://doi.org/10.1023/A:1025608728405.

Mohanty, A.K., Misra, M., Hinrichsen, G., 2000. Biofibres, biodegradable polymers and biocomposites: an overview. Macromol. Mater. Eng. 276–277, 1–24. https://doi.org/10.1002/(SICI)1439-2054(20000301)276:1<1::AID-MAME1>3.0.CO;2-W.

Mukherjee, S., Goulas, E., Creach, A., Krzewinski, F., Galinousky, D., Blervacq, A.-S., D'Arras, P., Ratahiry, S., Menuge, A., Soulat, D., Saliou, J.-M., Lacoste, A.-S., Hawkins, S., Grec, S., 2024. Metaproteomics identifies key cell wall degrading enzymes and proteins potentially related to inter-field variability in fiber quality during flax dew retting. Ind. Crop Prod. 222, 119907. https://doi.org/10.1016/j.indcrop.2024.119907.

Mukherjee, S., Goulas, E., De Waele, I., Créach, A., Hawkins, S., Grec, S., Blervacq, A.-S., 2025. Tracking flax dew retting by infrared vibrational spectroscopy combined with a powerful multivariate statistical analysis. Ind. Crop Prod. 227, 120798. https://doi.org/10.1016/j.indcrop.2025.120798.

Nykter, M., Kymäläinen, H.-R., Thomsen, A.B., Lilholt, H., Koponen, H., Sjöberg, A.-M., Thygesen, A., 2008. Effects of thermal and enzymatic treatments and harvesting time on the microbial quality and chemical composition of fibre hemp (*Cannabis sativa* L.). Biomass Bioenergy 32, 392–399. https://doi.org/10.1016/j.biombioe.2007.10.015.

Peyrache, T., Chabbert, B., Aguié-Béghin, V., Delattre, F., Kurek, B., Gainvors-Claisse, A., 2024. Multiscale assessment of the heterogeneity of scutched flax fibers. Ind. Crop Prod. 220, 119260. https://doi.org/10.1016/j.indcrop.2024.119260.

Réquilé, S., Mazian, B., Grégoire, M., Musio, S., Gautreau, M., Nuez, L., Day, A., Thiébeau, P., Philippe, F., Chabbert, B., Chamussy, A., Shah, D.U., Beaugrand, J., Placet, V., Benezet, J.-C., le Duigou, A., Bar, M., Malhautier, L., De Luycker, E., Amaducci, S., Baley, C., Bergeret, A., Bourmaud, A., Ouagne, P., 2021. Exploring the dew retting feasibility of hemp in very contrasting European environments: Influence on the tensile mechanical properties of fibres and composites. Ind. Crop Prod. 164, 113337. https://doi.org/10.1016/j.indcrop.2021.113337.

Rohart, F., Gautier, B., Singh, A., Cao, K.-A.-L., 2017. mixOmics: an R package for 'omics feature selection and multiple data integration. PLoS Comput. Biol. 13, e1005752. https://doi.org/10.1371/journal.pcbi.1005752.

Ruiz-Perez, D., Guan, H., Madhivanan, P., Mathee, K., Narasimhan, G., 2020. So you think you can PLS-DA? BMC Bioinf. 21, 2. https://doi.org/10.1186/s12859-019-3310-7.

Sanderson, K. (2015). A comparative study of handheld reflectance spectrophotometers. In: proceedings of the AIC annual meeting topics in photographic preservation (Vol. 16, pp. 47-62).

Seaby, D.A., Mercer, P.C., 1984. Development of a hand tool to test the degree of retting of flax straw. Ann. Appl. Biol. 104, 567–573. https://doi.org/10.1111/j.1744-7348.1984.tb03040.x.

Seymour, J., 2022. Color inconstancy in CIELAB: a red herring? Color Res. Appl. 47, 900–919. https://doi.org/10.1002/col.22782.

Sharma, G., Rodríguez-Pardo, C.E., 2012. The dark side of CIELAB, in: Color Imaging XVII: Displaying, Processing, Hardcopy, and Applications. Presented at the Color Imaging XVII: Displaying, Processing, Hardcopy, and Applications, SPIE, pp. 94–103. Doi: 10.1117/12.909960.

Sharma, H.S.S., Faughey, G.J., 1999. Comparison of subjective and objective methods to assess flax straw cultivars and fibre quality after dew-retting. Ann. Appl. Biol. 135, 495–501. https://doi.org/10.1111/j.1744-7348.1999.tb00879.x.

Sousa, C., 2022. Anthocyanins, Carotenoids and Chlorophylls in Edible Plant Leaves unveiled by Tandem Mass Spectrometry. Foods 11, 1924. https://doi.org/10.3390/foods11131924.

Suthar, M., Dufossé, L., Singh, S.K., 2023. The Enigmatic World of Fungal Melanin: a Comprehensive Review. Journal of Fungi 9, 891. https://doi.org/10.3390/jof9090891.

Szymańska, E., Saccenti, E., Smilde, A.K., Westerhuis, J.A., 2012. Double-check: validation of diagnostic statistics for PLS-DA models in metabolomics studies. Metabolomics 8, 3–16. https://doi.org/10.1007/s11306-011-0330-3.

Tariq, M., Khan, M.A., Muhammad, W., Ahmad, S., 2022. Fiber Crops in Changing Climate, in: Ahmed, M. (Ed.), Global Agricultural Production: Resilience to Climate Change. Springer International Publishing, Cham, pp. 267–282. Doi: 10.1007/978-3-031-14973-3_9.

Thapliyal, D., Verma, S., Sen, P., Kumar, R., Thakur, A., Tiwari, A.K., Singh, D., Verros, G.D., Arya, R.K., 2023. Natural fibers composites: origin, importance, consumption pattern, and challenges. J. Compos. Sci. 7, 506. https://doi.org/10.3390/jcs7120506.

Thiebeau, P., Recous, S., 2017. Dynamiques de décomposition des résidus de cultures sur des exploitations pratiquant l'agriculture de conservation en région Grand Est, France. Cah. Agric. 26, 65001. https://doi.org/10.1051/cagri/2017050.

Wang, Q., Chen, H., Fang, G., Chen, A., Yuan, P., Liu, J., 2017. Isolation of Bacillus cereus P05 and Pseudomonas sp. X12 and their application in the ramie retting. Ind. Crop Prod. 97, 518–524. https://doi.org/10.1016/j.indcrop.2016.12.047.

Xia, L., Lee, C., Li, J.J., 2024. Statistical method scDEED for detecting dubious 2D single-cell embeddings and optimizing t-SNE and UMAP hyperparameters. Nat. Commun. 15, 1753. https://doi.org/10.1038/s41467-024-45891-y.